GEM TN-91-28

Forward Calorimeter Transition, Z Position and Segmentation

G.E. Forden
University of Arizona

Abstract:

The transition between the End Cap calorimeter and the Plug calorimeter is investigated. There appears to be significant shower cross over, which can be diminished by end cap design. All three transition designs studied, however, produce effects which are small compared to irreducible neutrino background. The segmentation of a Plug calorimeter 6m from the interaction point is investigated and it is shown that this can be quite coarse.

AZPH-EX/91-31

Forward Calorimeter Transition, Z Position and Segmentation[1]

G. E. Forden
Department of Physics,University of Arizona
Tucson AZ 85721 USA

ABSTRACT

The transition between the End Cap calorimeter and the Plug calorimeter is investigated. There appears to be significant shower cross over, which can be diminished by End Cap design. All three transition designs studied, however, produce effects which are small compared to irreducible neutrino background. The segmentation of a Plug calorimeter 6m from the interaction point is investigated and it is shown that this can be quite coarse.

---

[1]To appear in the proceedings of Particles and Fields '91. Vancouver, British Columbia. August 18 - 22, 1991

Forward Calorimeter Transition, Z Position and Segmentation

G. E. Forden
Department of Physics,University of Arizona
Tucson AZ 85721 USA

ABSTRACT

The transition between the End Cap calorimeter and the Plug calorimeter is investigated. There appears to be significant shower cross over, which can be diminished by End Cap design. All three transition designs studied, however, produce effects which are small compared to irreducible neutrino background. The segmentation of a Plug calorimeter 6m from the interaction point is investigated and it is shown that this can be quite coarse.

1. η=3.0 Transition

Previous studies[1] have shown that SSC era calorimeters must cover the entire range of eta up to approximately 5 in order to see various missing P_t signatures, such as $H \rightarrow l^+l^- \nu \nu$. At the same time it was realized that the radiation environment and cost considerations combine to break the calorimeter at around η=3.0. The resulting calorimeter modules are often referred to as End Cap and Plug (or backstop) modules, as indicated in Fig. 1. This figure also shows the shower of a charged pion incident the End Cap near the transition region. This "shower cross over" is potentially a serious problem. The response of the calorimeter, as simulated by the SSCSIM[2] framework for the GEANT[3] shower Monte Carlo, is shown in Fig. 2. It is clear that the design of the calorimeter could minimize the effects of the shower cross over. Figure 3 shows the P_t response of an alternative design, which is shown schematically in the lower right hand corner. An additional alternative, one with a constant inner radius for the End Cap (often referred to as the "tube" design) gives qualitatively similar responses. These alternative designs have had the effect of changing the response of the calorimeter system, reducing the maximum effect of the shower cross over at the expense of distributing it over a wider range of η. However, in the physics signature used as a figure of merit, $H \rightarrow l^+l^- \nu \nu$, the missing P_t background induced by misestimated jets in this eta region is dominated by the irreducible background of neutrinos produced from heavy quark decay for all transition designs. Figure 4 shows the Pt jacobian peak for the observed Z^0 for a 400 GeV/c^2 Higgs and the background (mainly from Z^0 plus n QCD jets) as determined from a full simulation of the calorimeter response. The standard cone transition with

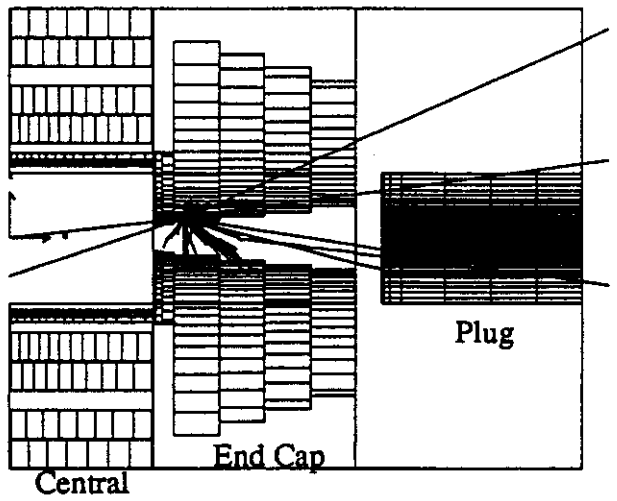

Figure 1. Half view of "standard cone" design calorimeter. Plug is 6 m from interaction point.

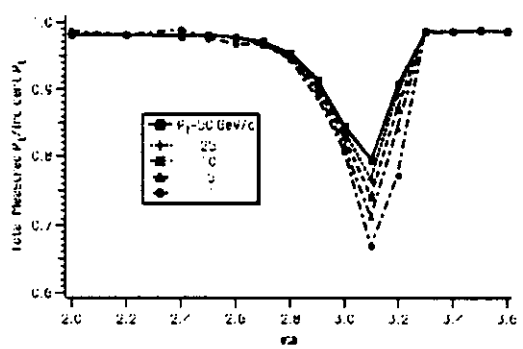

Figure 2. Relative Pt response of the standard cone to singlehadrons.

very thick walls (a total of 12 cm aluminum,) which functioned as a support structure as well as a cryostat, was also simulated. The P_t response for hadrons was similar to the response without walls provided an eta dependent calibration could be performed. This appears to be possible by extending work done for the DØ calorimeter calibration. The response to photons, however, was extremely poor with essentially total absorption over the eta range covered by the cryostat wall. Preliminary analysis of the effect of a magnetic field, as generated by a short solenoid, indicates that the shower cross over for hadrons is essentially undiminished.

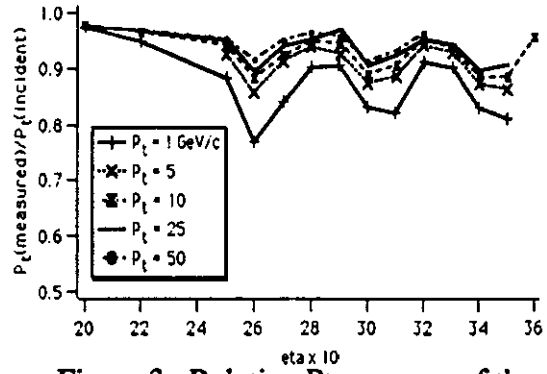

Figure 3. Relative Pt response of the "inverse cone" design. A silhouette of this design is shown in the lower right hand corner.

2. Forward Calorimeter Segmentation

There are many forces driving the position of the plug calorimeter inward. Chief among these is that the bulk cost (as opposed to the channel count cost) goes as the square of the z position. There are also forces driving the plug away from the the interaction point. These include the neutron albedo damage to the central tracker (as well as radiation concerns for the plug itself!) and a comparison of the $\Delta\eta \times \Delta\phi$ tower size to the characteristic physical shower dimension.. However, at the SSC it appears that only jets[4], as opposed to the single hadrons of the underlaying event, are important in determining the total Pt of the event. The segmentation issues become less clear when the goal is to determine the Pt of jets. A plug calorimeter design at 6 m and $\Delta\eta \times \Delta\phi = 0.1 \times 0.1$ with pseudo-projective towers (see Fig. 1) was simulated. The centroid of the jet was determined using only a single calorimeter layer and then the jet Pt was calculated as

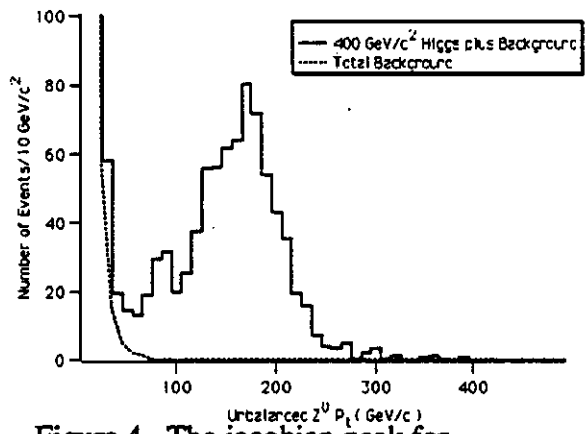

Figure 4. The jacobian peak for H →l+l- ν ν plus back ground.

$$P_t^L(\text{jet}) = \left(\sum_{\text{cells}}^{\text{all}} E_i \right) \cos\theta_L$$

where θ_L is the polar angle for the layer L's centroid. Figure 5 shows the average η projection of the jet energy profile for each layer. Superimposed on this is the energy profile, at layer 3 (which contains the electromagnetic shower maximum) for a typical jet. Figure 6 shows the error in determining η_{jet} made by choosing a particular layer for centroid determination (η_{jet}=3.6.) Only the

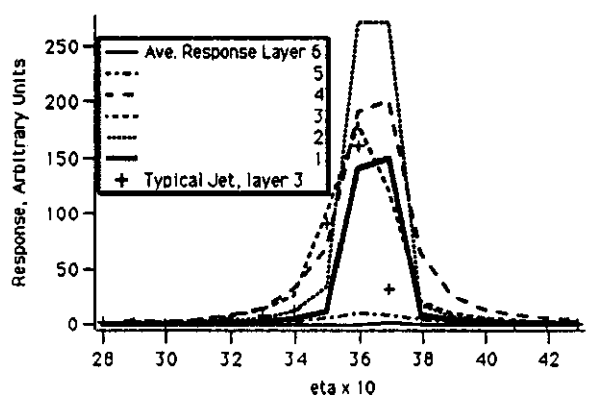

Figure 5. The average h projection of 100 GeV/c Pt jet (h=3.6.) A typical jet profile, for layer 3, is superimposed.

highest energy jets show any indication of their position resolution being dominated by the tower size. This improves, of course, for higher η. The actual error would also improve by including more than one psuedo-projective layer in the centroid determination. Figure 7 shows the relative Pt response of the calorimeter to jets using layer 3 for centroid determination and including only that energy within a cone of ΔR=0.7 in the jet energy sum. This can be directly compared to figure 2 which was for single particles. The average response shows a broad, but constant, transition effect. There is no apparent beam hole effect on the average response out to the highest h's studied. Figure 8, however, shows the RMS width of the average response and there is a clear rise in the jet Pt error near the beam pipe.

More work needs to be done in understanding the effect of this beam pipe on jet Pt measurements and how near to it is useful. It is clear that the segmentation of the plug calorimeter can be coarsened after the first absorption length with the resulting savings in channel count costs. The final physics limit on how coarse is acceptable will probably come from jet merging studies.

3. References

1. F. E. Paige, E. M. Wang, in *Workshop on Calorimetry for the Supercollider* R. Donaldson, M. G. D. Gilchriese, Eds. (World Scientific, Tuscaloosa AL, 1989), pp. 99.
2. S. Linn, *FSU-SCRI-90T-01* (1990).
3. R. Brun, F. Bruyant, M. Maire, A. C. Mcpherson, P. Zanarini, *DD/EE/84-1* (1987).
4. G. E. Forden, to appear in the Proceedings of *Workshop on Detector and Event Simulation in High Energy Physics* (World Scientific, Amsterdam, The Netherlands, 1991).

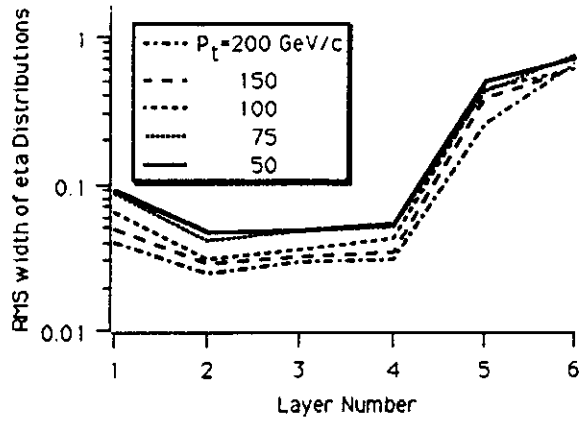

Figure 6. The RMS width of the jet eta distribution as determined for each layer. The incident jet η=3.6.

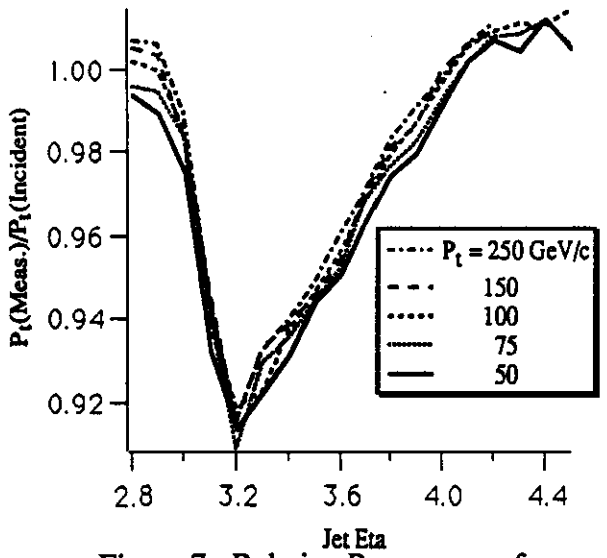

Figure 7. Relative P_t response of a ΔR=0.7 jet as a function of η.

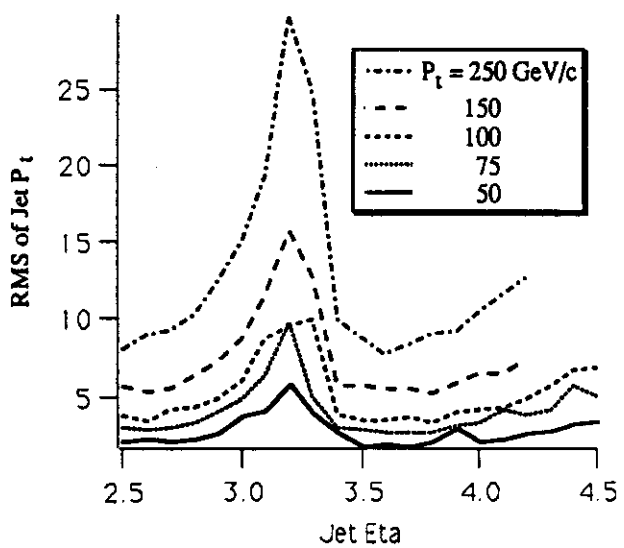

Figure 8. The RMS width of the reconstructed jet Pt distribution using layer 3 to determine the jet centroid.